On the Temperature Dependence of Amide I Frequencies of Peptides in Solution

Krista E. Amunson and Jan Kubelka*

Department of Chemistry, University of Wyoming, Laramie, Wyoming 82071

Received: March 29, 2007; In Final Form: June 8, 2007

The temperature dependence of the amide I vibrational frequencies of peptides in solution was investigated. In D_2O, the amide I′ bands of both an α-helical oligopeptide, the random-coil poly(L-lysine), and the simplest amide, *N*-methyl acetamide (NMA), exhibit linear frequency shifts of ∼0.07 $cm^{-1}/°C$ with increasing temperature. Similar amide I frequency shifts are also observed for NMA in both polar (acetonitrile and DMSO) and nonpolar (1,4-dioxane) organic solvents, thus ruling out hydrogen-bonding strength as the cause of these effects. The experimental NMA amide I frequencies in the organic solvents can be accurately described by a simple theory based on the Onsager reaction field with temperature-dependent solvent dielectric properties and a solute molecular cavity. DFT-level calculations (BPW91/cc-pVDZ) for NMA with an Onsager reaction field confirm the significant contribution of the molecular cavity to the predicted amide I frequencies. Comparison of the computations to experimental data shows that the frequency-dependent response of the reaction field, taken into account by the index of refraction, is crucial for describing the amide I frequencies in polar solvents. The poor predictions of the model for the NMA amide I band in D_2O might be due, in part, to the unknown temperature dependence of the refractive index of D_2O in the mid-IR range, which was approximated by the available values in the visible region.

Introduction

Infrared (IR) spectroscopy is widely used for experimental studies of peptide and protein structural changes due to thermal denaturation.[1] Most IR studies of peptide and protein structure focus on the amide I band (predominantly amide C═O bond stretching) as the sensitivity of this band to the protein secondary structure has been best established.[1−3] Traditionally, amide I frequencies are the basis for structural assignments, and amide I frequency shifts are the basis for the interpretation of structural changes. However, as we show in the following example, interpretation of the temperature-dependent amide I frequency shifts can be complicated by nonstructural effects, unrelated to the thermal unfolding of the peptide or protein structure.

Figure 1 shows the temperature dependence of the amide I′ (N-deuterated, in D_2O) peak frequencies for an alanine-rich α-helical peptide (AP21; for details, see Experiments). A cooperative helix-to-coil transition can be seen as a sigmoidal curvature of the temperature-dependent frequency shift. However, to fit the transition with the same thermodynamic parameters as obtained from the CD spectra of the same peptide,[4] linear temperature-dependent "baselines" for both the helix and coil state are necessary. These baselines, assumed to be the same for both states, indicate a blue shift of ∼6 cm^{-1} in the amide I′ frequency from 0 to 85 °C (∼0.07 $cm^{-1}/°C$).

The same frequency shift with increasing temperature is observed in the amide I′ band for poly(L-lysine) (PLL), also shown in Figure 1. PLL at neutral pH is one of the classic models for a random coil;[5−7] however, even in PLL, the melting of some residual structure cannot be completely excluded.[8] To decisively rule out the possibility of conformational transitions as sources of the temperature-dependent frequencies, we measured the amide I′ frequency as a function of temperature for *N*-methyl acetamide (NMA). Remarkably, the same frequency shift of the amide I′ maximum was observed yet again. Evidently, the amide I′ band of peptides in D_2O exhibits an intrinsic frequency shift with temperature, independent of structural changes.

The scope of this report is an investigation of the physical origin of these amide I′ vibrational frequency shifts with varying temperature. A likely explanation is interactions with the solvent, which have been firmly established to significantly influence the amide I frequencies. For example, in NMA, the amide I band shifts by as much as 100 cm^{-1} between the gas phase and aqueous solution.[9] In water, hydrogen bonding is the dominant cause for dramatically lower amide I frequencies. Even in nonprotic solvents, such as acetonitrile, the amide I frequencies shift substantially, presumably as a result of electrostatic interactions with the surrounding solvent.[9−11] Because both the strength of the hydrogen bonding and the dielectric properties of the solvent are temperature-dependent, the amide−solvent interaction can be expected to cause a shift in the amide I frequency with temperature.

Whereas numerous experimental and theoretical studies have focused on solvent effects on the amide I vibrational frequencies, in particular for NMA, their temperature dependence has received much less attention. Amide I frequency shifts with temperature have been observed for neat NMA[12−15] and for NMA in $CHCl_3$, where hydrogen-bonded NMA clusters are formed.[16] In aqueous solution (D_2O/glycerol), shifts in the amide I′ band of NMA were reported between ambient (290 K) and cryogenic (10 K) temperatures.[17] However, to our best knowledge, the temperature dependence of the amide I frequency of monomeric NMA in solution has not been investigated within the range of temperatures most relevant to protein thermal denaturation studies, i.e., 0−100 °C.

In the above-cited reports, the amide I frequency shifts were generally attributed to an increased strength of hydrogen bonding, either between the individual NMA molecules (neat

* Corresponding author. E-mail: jkubelka@uwyo.edu.

10.1021/jp072454p CCC: $37.00
Published on Web 08/03/2007

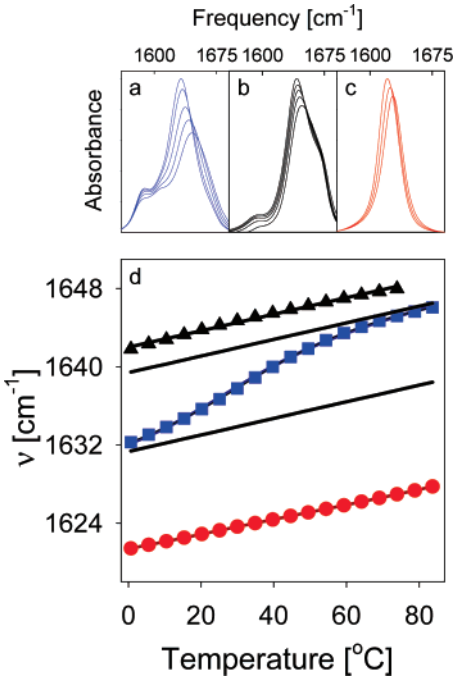

Figure 1. Temperature dependence of the amide I′ vibrational frequencies of peptides in D_2O. FTIR amide I′ bands of (a) alanine-rich peptide AP21 at (nominally) 0, 15, 35, 55, and 85 °C; (b) poly-(L-lysine) (PLL) at neutral pH at 0, 10, 25, 45, and 75 °C; and (c) *N*-methyl acetamide (NMA) at 0, 45, and 85 °C. (d) Peak amide I′ frequencies as a function of temperature, where the experimental data for AP21 (blue squares) are fitted to a two-state helix−coil transition model with the thermodynamic parameters obtained from the circular dichroism (CD) data for this peptide. The solid black lines are the resulting temperature-dependent baselines for the helix and coil states. The experimental amide I′ peak frequencies of PLL (black triangles) and NMA (red circles) are shown with linear fits to the data.

NMA and NMA clusters in $CHCl_3$) or between the NMA molecules and the solvent (D_2O). As we show in the following discussion, hydrogen bonding cannot provide the whole explanation, because frequency shifts similar to those observed in aqueous solution (Figure 1) are found in non-hydrogen-bonding solvents. Furthermore, we demonstrate that these temperature-dependent amide I frequencies can be quantitatively explained by a simple solvent model based on the reaction field of the dielectric continuum. These observations are important for understanding solvent effects on the amide vibrational frequencies, which is necessary for the proper structural interpretation of experimental peptide and protein IR spectra.

Materials and Methods

Experiments. All solvents used in this study were of analytical or better grade. Poly(L-lysine) (PLL) and *N*-methyl acetamide (NMA) were purchased from Sigma-Aldrich; D_2O was obtained from Cambridge Isotope Laboratories. AP21 peptide (Ac−AAAAAAAARAAAARAAAARAA−NH_2, Ac = acetate, A = alanine, R = arginine) was synthesized using a standard FMOC solid-phase synthesis on a PS-3 automated peptide synthesizer (Protein Technologies Inc.) and purified by HPLC to >95% purity, as verified by mass spectrometry.

Both AP21 and PLL were pre-exchanged with deuterium by dissolving the samples in D_2O and then subjecting them to lyophilization. FTIR spectra of PLL and AP21 were collected at a concentration of ~20 mg/mL. PLL was dissolved in a 50 mM phosphate buffer, pH 6.9, to ensure the random-coil conformation.[5−7] AP21 was dissolved in D_2O. Samples of NMA in D_2O and 1,4-dioxane were prepared at a concentration of 10 mg/mL; in acetonitrile and DMSO, the NMA concentration was 5 mg/mL.

All FTIR spectra were measured on a Bruker Tensor 27 spectrometer equipped with an RT-DLaTGS detector. The samples were placed in a custom-made IR cell with CaF_2 windows and 50- or 100-μm Teflon spacers. A total of 256 scans at a resolution of 4 cm^{-1} were collected. The temperature was controlled by an external water bath interfaced with the FTIR control software. For all samples, the spectra were collected in 5 °C increments. The temperature ranges varied because of differences in the melting and boiling points of the different solvents and were (nominally) as follows: D_2O, 0−85 °C; acetonitrile, 0−80 °C; DMSO and 1,4-dioxane, 10−85 °C. The exact temperature of the sample was monitored using a thermocouple. The spectra of the various solvents were collected under identical conditions and subtracted from those of the corresponding samples.

The analysis and fitting of the experimental data was performed using Matlab (Mathworks, Inc.). The peak amide I/I′ frequencies were found from the zero crossings of the first-derivative spectra. The temperature-dependent dielectric constants and indices of refraction for D_2O, 1,4-dioxane, acetonitrile, and DMSO and the density of NMA were compiled from the available literature data.[18−22] Linear or quadratic regression was used to interpolate and/or extrapolate over the temperature ranges used in our experiments. The values of all material constants used in this study are listed in Table 1.

Computations. Density functional theory (DFT) calculations of NMA vibrational frequencies were performed using Gaussian 03[23] with an Onsager reaction field. A BPW91[24,25] density functional with a cc-pVDZ basis set[26] was used, because this level most accurately reproduces the gas-phase NMA amide I frequency.[9] Prior to each frequency calculation, the NMA molecule was fully optimized to the default Gaussian 03 criteria at the same level of theory. The calculations were carried out on the NCSA (National Center for Supercomputing Applications) SGI Altix cluster through an allocation provided by the NSF Teragrid program.

Results and Discussion

As shown in Figure 1, the amide I′ band of NMA in D_2O exhibits a frequency shift of 6 cm^{-1} between 0 and 85 °C, or about 0.07 cm^{-1}/°C. Generally, frequency shifts with temperature in neat NMA[12−15] and NMA solutions in $CHCl_3$[16] and

TABLE 1: Material Constants Used in the Analysis of the Temperature-Dependent NMA Amide I Frequency Shifts

solvent	ϵ (20 °C)	$d\epsilon/dT$ (°C^{-1})	$d^2\epsilon/dT^2$ (°C^{-2})	n (20 °C)	dn/dT (°C^{-1})	d^2n/dT^2 (°C^{-2})	ρ (30 °C) (g cm^{-3})	$d\rho/dT$ (g cm^{-3} °C^{-1})
DMSO[a]	47.397	-8.9540×10^{-2}	-4.74×10^{-4}	1.4793	-4.6037×10^{-4}	-2.66×10^{-7}		
acetonitrile	36.804[b]	-1.6993×10^{-1}		1.3437[c]	-4.8350×10^{-4}			
1,4-dioxane	2.2175[b]	-1.71×10^{-3}		1.4207[c]	-4.6894×10^{-4}	-3.75×10^{-8}		
D_2O[e]	79.755	-3.984×10^{-1}	7.84×10^{-4}	1.3283	-1.5371×10^{-4}			
NMA							0.9502[c]	-8.383×10^{-4}

[a] Reference 22. [b] Reference 21. [c] Reference 20. [d] Reference 19. [e] Reference 18.

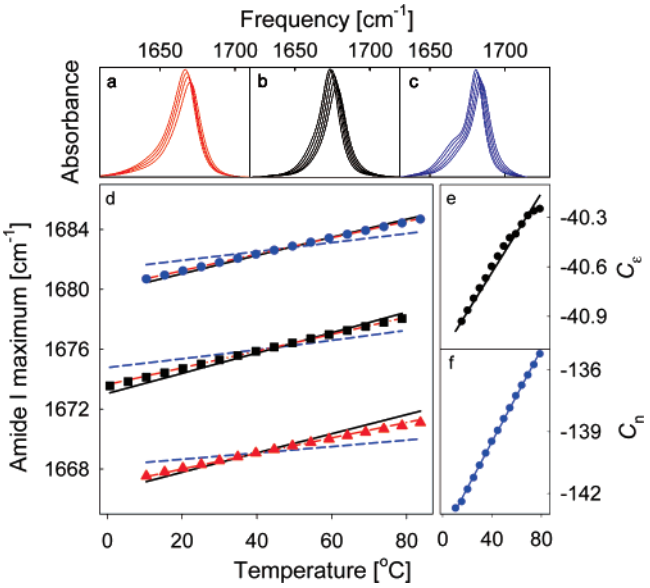

Figure 2. Experiment and theory for the temperature dependence of the amide I vibrational frequencies of *N*-methyl acetamide (NMA) in organic solvents. FTIR amide I bands of NMA in (a) DMSO at (nominally) 10, 30, 50, and 80 °C; (b) acetonitrile at 0, 20, 40, 60, and 80 °C; and (c) 1,4-dioxane at 10, 25, 45, 65, and 85 °C. (d) Peak amide frequencies for DMSO (red triangles), acetonitrile (black squares), and 1,4-dioxane (blue circles). The blue dashed line represents the least-squares fit to eq 1 with temperature-independent coefficients C_ϵ and C_n. The red dash-dotted line is the fit to eq 1 using temperature-dependent parameters $C_\epsilon(T)$ and $C_n(T)$ that correspond, respectively, to the straight lines in plots e and f. These lines are the results of a linear regression to the sets of constants (circles in e and f) obtained from eq 1 for all three solvents simultaneously, but independently, at each temperature and with the gas-phase frequency (ν_0) constrained to be the same for all temperatures. The solid black line in d is the best fit to eq 2 using temperature-dependent cavity radius calculated from the NMA density using eq 3 and constant C'_ϵ and C'_n.

D_2O/glycerol (10−290 K)[17] have been attributed to hydrogen bonding. To test whether the observed amide I′ shift is likewise due to hydrogen bonding with D_2O, we measured the amide I band of NMA as a function of temperature in several non-hydrogen-bonding solvents, namely, DMSO, acetonitrile, and 1,4-dioxane. The results are shown in Figure 2 and summarized in Table 2.

The NMA amide I bands in DMSO, acetonitrile, and 1,4-dioxane exhibit linear frequency shifts of 4−5 cm^{-1} within the measured temperature ranges, with slopes of 0.05−0.06 cm^{-1}/°C. Therefore, even in non-hydrogen-bonding solvents, the changes with temperature of the NMA amide I frequency are very similar to and only slightly smaller than those measured in D_2O.

In the absence of hydrogen bonding, the variations in the amide I vibrational frequency must be due to changes in the dielectric properties of the solvent. To quantitatively test this hypothesis, we used the theory derived by Buckingham,[27] which is based on the simplest model for the solvent electrostatic effects, the Onsager reaction field[28]

$$\nu = \nu_0 + C_\epsilon \frac{\epsilon - 1}{2\epsilon + 1} + C_n \frac{n^2 - 1}{2n^2 + 1} \qquad (1)$$

In eq 1, ν is the vibrational frequency in solution; ν_0 is the gas-phase frequency; ϵ is the dielectric constant; n is the refractive index; and C_ϵ and C_n are constants characteristic of the given solute, in this case NMA. Rigorously, the refractive indices at the amide I vibrational frequencies (in the IR range) are needed in eq 1. Unfortunately, temperature-dependent data could be found only for refractive indices in the visible region (Table 1). This should not represent a major problem for solvents with little or no absorption (and therefore anomalous dispersion) in the vicinity of the NMA amide I band, where the refractive index in the visible region should be the same as in the IR region.[29] For aqueous solutions, however, this can present a major caveat (see discussion below).

Figure 2d shows the results of fitting the temperature-dependent NMA amide I frequencies in the three organic solvents with eq 1, using the temperature-dependent dielectric constants ϵ and indices of refraction n (Table 1). With constant C_ϵ and C_n, the temperature dependence of the peak amide I vibrational frequencies is poorly reproduced by eq 1 (blue dashed lines). By contrast, an excellent fit to the data is obtained (Figure 2d, red dash-dotted line) with linearly temperature-dependent coefficients, denoted $C_\epsilon(T)$ and $C_n(T)$ and plotted in Figure 2e and f, respectively. The resulting extrapolated gas-phase frequency ν_0 is 1719 cm^{-1}, which is very close to the experimental amide I frequency of NMA in the gas phase of 1722 cm^{-1}. (In the gas phase, the NMA amide I is a doublet[13] with peak maxima at 1731 and 1714 cm^{-1}. We assume the true ν_0 to be the average, 1722 cm^{-1}.)

To find the physical explanation for the temperature dependence of the molecular constants $C_\epsilon(T)$ and $C_n(T)$, we rewrite eq 1 as

$$\nu = \nu_0 + C'_\epsilon \frac{\epsilon - 1}{2\epsilon + 1}\frac{1}{a^3} + C'_n \frac{n^2 - 1}{2n^2 + 1}\frac{1}{a^3} \qquad (2)$$

where a is the radius of the spherical solute molecular cavity in the Onsager reaction field model and the new molecular constants are $C'_\epsilon = C_\epsilon a^3$ and $C'_n = C_n a^3$. While there is no rigorous way to calculate the cavity dimensions,[30−32] according

TABLE 2: Experimental NMA Amide I/I′ Frequencies in Different Solvents and Parameters of the Theoretical Model

solvent	T_{min},[a] T_{max} (°C)	$\tilde{\nu}(T_{min})$, $\tilde{\nu}(T_{max})$, (cm^{-1})	$d\tilde{\nu}/dT$ (cm^{-1} °C^{-1})	C_ϵ (20 °C) (cm^{-1}),[b] dC_ϵ/dT (cm^{-1} °C^{-1})	C_n (20 °C) (cm^{-1}),[b] dC_n/dT (cm^{-1} °C^{-1})	C'_ϵ (cm^{-1} $Å^{-3}$)[c]	C'_n (cm^{-1} $Å^{-3}$)[c]
DMSO	10.5	1667.5	0.05				
	83.7	1671.1					
acetonitrile	0.7	1673.6	0.06	-4.087×10^1	-1.418×10^2		
	78.8	1678.0				-6.217×10^2	-2.094×10^3
1,4-dioxane	10.5	1680.7	0.05	1.2×10^{-2}	1.12×10^{-1}		
	83.7	1684.7					
D_2O	0.7	1621.4	0.07				
	83.7	1627.7					

[a] Calibrated temperatures. [b] Temperature-dependent coefficients from the best fit of eq 1 to the experimental NMA amide I frequencies in DMSO, acetonitrile, and 1,4-dioxane. The extrapolated gas-phase amide I frequency is $\nu_0 = 1719.1$ cm^{-1}. [c] Coefficients from the best fit of eq 2 to the experimental NMA amide I frequencies in DMSO, acetonitrile, and 1,4-dioxane, with the molecular cavity radii calculated from eq 3 and the temperature-dependent NMA density ρ (Table 1). The extrapolated gas-phase amide I frequency is $\nu_0 = 1718.3$ cm^{-1}.

to Onsager's original suggestion,[33] the cavity radius a can be estimated from the solute molar volume as

$$V_m = \frac{M_m}{\rho} = \frac{4}{3} N_A \pi a^3 \quad (3)$$

where ρ is the density, M_m is the molar mass, and N_A is Avogadro's constant. From eq 3, $1/a^3 \propto \rho$, and ρ is, in general, temperature-dependent. The parameters C'_ϵ and C'_n in eq 2 now depend only on the fundamental constants and molecular constants of the solute and should be independent of temperature.

With the simplest possible estimate of the temperature-dependent radius a from eq 3 using the density of neat NMA (Table 1), we used eq 2 to again fit the experimental NMA amide I data in the three solvents. As shown in Figure 2d (solid black line), this fit is somewhat worse (rms deviation of 1.7 cm^{-1}) than the fit with the "empirical" temperature dependence of the molecular constants (red dash-dotted line, rms deviation of 0.4 cm^{-1}) and slightly overestimates the temperature-induced frequency shift, especially for the polar solvents acetonitrile and DMSO. That the predicted temperature dependence is stronger than observed is consistent with the estimate of the molecular volume based on neat NMA, which is significantly more polar than any of the studied solvents and forms strongly hydrogen-bonded networks. Weaker interactions of NMA with DMSO, acetonitrile, and 1,4,-dioxane would yield a weaker temperature dependence of the local solvent density around the NMA molecules. Overall, considering this relatively crude approximation for the molecular cavity, eq 2 yields a very satisfactory fit to the experimental data. The decrease of the solution density with temperature, therefore, provides a simple and quantitative explanation for the temperature dependence of the molecular constants in eq 1.

To explore the effect of the molecular cavity radius in even more depth, we simulated the NMA amide I frequencies in different solvents and at different temperatures using DFT (BPW91/cc-pVDZ) calculations with the Onsager reaction field. Two sets of calculations were performed at five temperature points over the range of experimental temperatures. First, the dielectric constants were set to the experimental values for 1,4-dioxane, acetonitrile, and DMSO, but the cavity radius was fixed to the value for the optimized gas-phase NMA. Second, the same dielectric constants were used, but the cavity radius was assumed to change with temperature according to eq 3 and the literature data for neat NMA density (Table 1). The results of the simulations are listed in Table 3.

Using only the temperature dependence of ϵ and a constant cavity radius yields essentially temperature-independent amide I frequencies. By contrast, with the cavity radius increasing with temperature as estimated from the NMA density, significant amide I frequency shifts with temperature are predicted. For 1,4-dioxane, the computed frequency shift (0.04 cm^{-1}/°C) is very close to that measured experimentally (0.05 cm^{-1}/°C), whereas for acetonitrile and DMSO, even greater frequency shifts are computed (0.15 cm^{-1}/°C) than measured (0.06 cm^{-1}/°C). These results qualitatively agree with the empirical fit of eq 2, with the same estimate for the NMA molecular radius, which also overestimated the temperature dependence of the amide I frequencies in acetonitrile and DMSO. However, both sets of calculations fail to reproduce the relative amide I frequencies in the solvents of different polarity. In particular, the amide I frequencies computed for NMA in the two polar solvents, acetonitrile and DMSO, are within 1−2 cm^{-1}.

TABLE 3: Temperature Dependence of NMA Amide I Frequencies (cm^{-1}) Calculated at the DFT BPW91/cc-pVDZ Level with the Onsager Reaction Field Model for Different Solvents[a]

temperature[b] (°C):	0.7	20.2	39.8	59.3	78.8
cavity radius (Å):			3.54[c]		
DMSO	1666.5	1666.1	1666.2	1666.3	1666.4
acetonitrile	1666.9	1666.8	1667.1	1667.3	1667.4
1,4-dioxane	1701.8	1702.0	1702.2	1702.5	1702.7
temperature[b] (°C):	0.7	20.2	39.8	59.3	78.8
cavity radius[d] (Å):	3.18	3.20	3.22	2.23	3.25
DMSO	1628.0	1630.6	1634.3	1637.4	1639.3
acetonitrile	1630.0	1632.4	1634.0	1638.1	1641.5
1,4-dioxane	1691.5	1692.3	1693.1	1693.9	1694.7

[a] Calculations performed using temperature-dependent dielectric constants for the individual solvents (Table 1) [b] Temperatures corresponding to the calibrated experimental temperature points. [c] Cavity radius calculated from a fully optimized gas-phase NMA volume at the BPW91/cc-pVDZ level (Gaussian 03 default for Onsager reaction field calculations). [d] Cavity radius calculated from eq 3 and NMA density data (Table 1).

The reason for the temperature-independent amide I frequencies computed with the fixed cavity radius is that, for ϵ significantly greater than 1, the factor $(\epsilon - 1)/(2\epsilon + 1)$ becomes nearly independent of ϵ. Therefore, relatively small changes of ϵ with temperature do not significantly affect the magnitude of the reaction field. For that same reason, the reaction field of acetonitrile ($\epsilon \approx 35$) is nearly the same as that of DMSO ($\epsilon \approx 45$), yielding much smaller differences in the amide I frequencies than seen experimentally in these two solvents. On the other hand, the reaction field is strongly dependent on the cavity radius (inverse third power). We note that this effect is not limited to the simple Onsager model. Similar calculations with the more realistic polarized continuum model (PCM)[34−36] yielded exactly the same trends: for $\epsilon \geq 30$, the computed frequencies were virtually independent of changes in ϵ, but they were significantly affected by variations in the size of the atomic radii.

The failure of the calculations to reproduce the different amide I frequencies in acetonitrile and DMSO underscores the importance of the last term in eqs 1 and 2, which represents the frequency-dependent response of the reaction field.[27] The implicit solvent models used for quantum mechanical calculations do not include this contribution; they include only the static dielectric constant. On the other hand, with both static and frequency-dependent terms, the Buckingham model can accurately explain the absolute experimental NMA amide I frequencies in different solvents over a broad temperature range and can even predict the correct gas-phase frequency. We stress this point especially because numerous models that have recently been developed for solvent effects on the amide I frequencies are based solely on static electric fields.[10,11,37,38]

Finally, we return to the amide I′ vibrational frequencies in D_2O, which is the most relevant solvent for studies of peptides and proteins. In Figure 3, we show the predictions of the Buckingham theory using the temperature-dependent values ϵ and n for D_2O (Table 1). Two theoretical curves are calculated with the same parameters that gave the best fits to the data for the three organic solvents: the first using eq 1 with the empirical temperature dependence of $C_\epsilon(T)$ and $C_n(T)$ and the second using eq 2 with the temperature-dependent molecular radius a calculated from eq 3 and the NMA density.

The amide I frequencies predicted by the model for a D_2O solution are overall much higher, by about 50 cm^{-1}, than the experimental values. This is not surprising, because the much

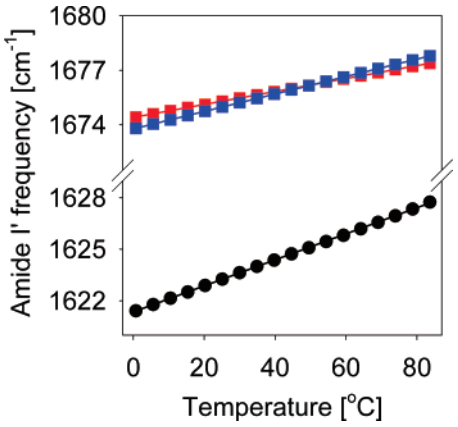

Figure 3. Prediction of the model for the temperature dependence of the NMA amide I′ vibrational frequencies in D_2O using the parameters that yielded the best fits to the NMA amide I in the three organic solvents (Figure 2, Table 2). The black circles are the experimental peak amide I′ frequencies, the blue squares are the amide I frequencies predicted by eq 1 with temperature-dependent constants $C_\epsilon(T)$ and $C_n(T)$ (Figure 2e,f), and the red squares are the frequencies calculated from eq 2 with the temperature-dependent molecular radius for NMA according to eq 3.

lower experimental frequencies in D_2O are in large part due to hydrogen bonding,[9] which is not taken into account in the model. However, the model also underestimates the temperature dependence of the amide I′ frequency in D_2O. Experimentally, the amide I′ shifts by slightly more than 6 cm^{-1} between 0 and 85 °C, with a derivative of 0.07 cm^{-1}/°C. The predictions yield only a 3 cm^{-1} shift (0.04 cm^{-1}/°C) for the model with empirical temperature-dependent molecular constants (eq 1) and 4 cm^{-1} (0.05 cm^{-1}/°C) for eq 2 with the temperature-dependent NMA molecular radius.

An obvious explanation for this discrepancy is that the simple form of eq 1 is not expected to work for hydrogen-bonding solvents,[27] where higher-order terms in ϵ and n can become significant. We could even argue that the excess temperature shift of the amide I′ frequency in D_2O that is not predicted by the model is due to the temperature dependence of the hydrogen-bonding strength.[17] However, another reason might be the refractive index of D_2O in the mid-IR region. As discussed above, within the limits of the Buckingham theory, the index of refraction is crucial for explaining the amide I frequency shifts due to both the solvent and the temperature, especially in polar solvents. The refractive index n of D_2O in the mid-IR range has been measured at 22 °C,[39] but its temperature dependence in the IR region is not known. Therefore, we used the data in the visible region,[18] where the n value of D_2O is relatively weakly temperature-dependent. In the IR region, however, D_2O has strong absorption bands, and the corresponding anomalous dispersion of the refractive index spans the amide I region.[39] Because the strong stretching (~2500 cm^{-1}) and bending (~1210 cm^{-1}) absorption bands are temperature-dependent, the refractive index will be as well. An additional contribution might arise from the dispersion associated with the combination band of the D_2O bending and libration modes (~1550 cm^{-1}), which partially overlaps the amide I region and shifts considerably with temperature.

At this point, unfortunately, we can only speculate that a more strongly temperature-dependent refractive index of D_2O in the IR range might improve the predictions of the Buckingham formula for the amide I frequency shifts in D_2O. Measurements of the temperature-dependent refractive indices for H_2O and D_2O in the mid-infrared region are currently underway in our laboratory. Our future research will also focus on studies of solvent- and temperature-induced changes in the amide absorption intensities and band widths. Understanding the solvent and temperature effects on all amide I spectral features is critical for a reliable interpretation of peptide and protein vibrational spectra in terms of structure and structural changes.

Conclusion

We have shown that the IR amide I/I′ band of peptides in solution exhibits frequency shifts with temperature as a result of temperature-dependent solvent effects. The amide I frequency shifts with varying temperature in D_2O cannot be entirely due to hydrogen bonding, but rather arise from the temperature dependence of the solvent dielectric properties. A simple theory based on the Onsager reaction field is remarkably successful in describing the NMA amide I frequencies for a range of solvents and temperatures. The success of this simple model is encouraging, as it can provide an understanding of solvent effects on vibrational spectra based only on macroscopic solvent properties: dielectric constant, index of refraction, and density. In particular, our results highlight the importance of the index of refraction, which represents the frequency-dependent response of the reaction field to the molecular oscillator. This is an important observation, because numerous more involved, molecular-level models for solvent effects on amide vibrational spectra are based only on static electric fields. Although the temperature dependence of the refractive indices for water and D_2O in the mid-IR region is as yet unknown, it might be significant and might influence the amide I spectra more dramatically than is currently appreciated. This underlines the importance of studying the temperature-dependent properties of H_2O and D_2O in the IR region and relating these properties to vibrational spectral changes. Understanding the nonstructural effects in vibrational spectra is necessary for IR spectroscopy to be a useful quantitative tool for investigating protein structures and structural transitions.

Acknowledgment. This work was supported by the Faculty Grant-in-Aid and Basic Research Grant programs of the University of Wyoming. The computations were made possible by the National Science Foundation under the following NSF programs: Partnerships for Advanced Computational Infrastructure, Distributed Terascale Facility (DTF), and Terascale Extensions: Enhancements to the Extensible Terascale Facility.

References and Notes

(1) Barth, A.; Zscherp, C. *Q. Rev. Biophys.* **2002**, *35*, 369.
(2) Haris, P. I. Fourier Transform Infrared Spectroscopic Studies of Peptides: Potentials and Pitfalls. In *Infrared Analysis of Peptides and Proteins: Principles and Applications*; Ram Singh, B., Ed.; ACS Symposium Series; American Chemical Society: Washington, DC, 2000; p 54.
(3) Goormaghtigh, E.; Cabiaux, V.; Ruysschaert, J. M. Determination of soluble and membrane protein structure by Fourier transform infrared spectroscopy. I. Assignments and model compounds. In *Subcellular Biochemistry*; Hilderson, H. J., Ralston, G. B., Eds.; Plenum Press: New York, 1994, Vol. 23, p 329.
(4) Murza, A. C.; Kubelka, J., manuscript in preparation.
(5) Susi, H.; Timasheff, S. N.; Stevens, L. *J. Biol. Chem.* **1967**, *242*, 5460.
(6) Fasman, G. D. *Poly-α-Amino Acids: Protein Models for Conformational Studies*; Marcel Dekker, Inc.: New York 1967.
(7) Holzwarth, G.; Doty, P. *J. Am. Chem. Soc.* **1965**, *87*, 218.
(8) Shi, Z. S.; Woody, R. W.; Kallenbach, N. R. *Adv. Protein Chem.* **2002**, *62*, 163.
(9) Kubelka, J.; Keiderling, T. A. *J. Phys. Chem. A* **2001**, *105*, 10922.
(10) Jansen, T. L.; Knoester, J. *J. Chem. Phys.* **2006**, *124*, 044502.
(11) DeCamp, M. F.; DeFlores, L.; McCracken, J. M.; Tokmakoff, A.; Kwac, K.; Cho, M. *J. Phys. Chem. B* **2005**, *109*, 11016.

(12) Whitfield, T. W.; Martyna, G. J.; Allison, S.; Bates, S. P.; Vass, H.; Crain, J. *J. Phys. Chem. B* **2006**, *110*, 3624.
(13) Czarnecki, M. A.; Haufa, K. Z. *J. Phys. Chem. A* **2005**, *109*, 1015.
(14) Huang, H.; Malkov, S.; Coleman, M.; Painter, P. *J. Phys. Chem. A* **2003**, *107*, 7697.
(15) Herrebout, W. A.; Clou, K.; Desseyn, H. O. *J. Phys. Chem. A* **2001**, *105*, 4865.
(16) Ludwig, R.; Reis, O.; Winter, R.; Weinhold, F.; Farrar, T. C. *J. Phys. Chem. B* **1998**, *102*, 9312.
(17) Manas, E. S.; Getahun, Z.; Wright, W. W.; Degrado, W. F.; Vanderkooi, J. M. *J. Am. Chem. Soc.* **2000**, *122*, 9883.
(18) Lide, D. R., Ed. *CRC Handbook of Chemistry and Physics*, 84th ed.; CRC Press LLC: Boca Raton, FL, 2003.
(19) *Perry's Chemical Engineer's Handbook*, 7th ed.; McGraw-Hill: New York, 1997.
(20) Lide, D. R., Ed. *CRC Handbook of Thermophysical and Thermochemical Data*; CRC Press: Boca Raton, FL, 1994.
(21) Pacak, P. *Chem. Pap.* **1991**, *45*, 227.
(22) Bicknell, R. T. M.; Davies, D. B.; Lawrence, K. G. *J. Chem. Soc., Faraday Trans. 1* **1982**, *78*, 1595.
(23) Frisch, M. J.; Trucks, G. W.; Schlegel, H. B.; Scuseria, G. E.; Robb, M. A.; Cheeseman, J. R.; Zakrzewski, V. G.; Montgomery, J. A., Jr.; Stratmann, R. E.; Burant, J. C.; Dapprich, S.; Millam, J. M.; Daniels, A. D.; Kudin, K. N.; Strain, M. C.; Farkas, O.; Tomasi, J.; Barone, V.; Cossi, M.; Cammi, R.; Mennucci, B.; Pomelli, C.; Adamo, C.; Clifford, S.; Ochterski, J.; Petersson, G. A.; Ayala, P. Y.; Cui, Q.; Morokuma, K.; Malick, D. K.; Rabuck, A. D.; Raghavachari, K.; Foresman, J. B.; Cioslowski, J.; Ortiz, J. V.; Stefanov, B. B.; Liu, G.; Liashenko, A.; Piskorz, P.; Komaromi, I.; Gomperts, R.; Martin, R. L.; Fox, D. J.; Keith, T.; Al-Laham, M. A.; Peng, C. Y.; Nanayakkara, A.; Gonzalez, C.; Challacombe, M.; Gill, P. M. W.; Johnson, B.; Chen, W.; Wong, M. W.; Andres, J. L.; Gonzalez, C.; Head-Gordon, M.; Replogle, E. S.; Pople, J. A. *Gaussian 03*; Gaussian, Inc.: Pittsburgh, PA, 2003.
(24) Becke, A. D. *J. Chem. Phys.* **1993**, *98*, 5648.
(25) Perdew, J. P.; Wang, Y. *Phys. Rev. B* **1992**, *45*, 13244.
(26) Dunning, T. H. *J. Chem. Phys.* **1989**, *90*, 1007.
(27) Buckingham, A. D. *Proc. R. Soc. London A* **1958**, *248*, 169.
(28) Onsager, L. *J. Am. Chem. Soc.* **1936**, *58*, 1486.
(29) Person, W. B. *J. Chem. Phys.* **1958**, *28*, 319.
(30) Zhan, C. G.; Chipman, D. M. *J. Chem. Phys.* **1998**, *109*, 10543.
(31) Luo, Y.; Agren, H.; Mikkelsen, K. V. *Chem. Phys. Lett.* **1997**, *275*, 145.
(32) Linder, B.; Hoernsch.D. *J. Chem. Phys.* **1967**, *46*, 784.
(33) Onsager, L. *J. Am. Chem. Soc.* **1936**, *58*, 1486.
(34) Cossi, M.; Scalmani, G.; Rega, N.; Barone, V. *J. Chem. Phys.* **2002**, *117*, 43.
(35) Mennucci, B.; Tomasi, J. *J. Chem. Phys.* **1997**, *106*, 5151.
(36) Tomasi, J.; Persico, M. *Chem. Rev.* **1994**, *94*, 2027.
(37) Hayashi, T.; Zhuang, W.; Mukamel, S. *J. Phys. Chem. A* **2005**, *109*, 9747.
(38) Bour, P. *J. Chem. Phys.* **2004**, *121*, 7545.
(39) Bertie, J. E.; Ahmed, M. K.; Eysel, H. H. *J. Phys. Chem.* **1989**, *93*, 2210.